Cell PRESS
Developmental Cell
Article

The Arp2/3 Activator WASH Controls the Fission of Endosomes through a Large Multiprotein Complex

Emmanuel Derivery,[1,2,3] Carla Sousa,[3] Jérémie J. Gautier,[3] Bérangère Lombard,[1] Damarys Loew,[1] and Alexis Gautreau[1,2,3,*]
[1]Institut Curie, Centre de Recherche
[2]CNRS UMR144
26 rue d'Ulm, 75248 Paris Cedex 05, France
[3]CNRS UPR3082, Laboratoire d'Enzymologie et de Biochimie Structurales, Bât. 34 Avenue de la Terrasse, 91198 Gif-sur-Yvette Cedex, France
*Correspondence: alexis.gautreau@lebs.cnrs-gif.fr
DOI 10.1016/j.devcel.2009.09.010

SUMMARY

The Arp2/3 complex generates branched actin networks when activated by Nucleation Promoting Factors (NPFs). Recently, the WASH family of NPFs has been identified, but its cellular role is unclear. Here, we show that WASH generates an actin network on a restricted domain of sorting and recycling endosomes. We found that WASH belongs to a multiprotein complex containing seven subunits, including the heterodimer of capping protein (CP). In vitro, the purified WASH complex activates Arp2/3-mediated actin nucleation and binds directly to liposomes. WASH also interacts with dynamin. WASH depletion gives rise to long membrane tubules pulled out from endosomes along microtubules, as does dynamin inhibition. Accordingly, WASH is required for efficient transferrin recycling. Together, these data suggest that the WASH molecular machine, integrating CP with a NPF, controls the fission of endosomes through an interplay between the forces generated by microtubule motors and actin polymerization.

INTRODUCTION

The actin cytoskeleton is a dynamic ensemble of microfilaments that contributes to cell morphogenesis. The polarized assembly of actin filaments often occurs at the surface of membranes, developing forces that cause their deformation or movement. Several classes of actin nucleators initiate these actin-based processes (Pollard, 2007). Among these, the Arp2/3 complex both nucleates and organizes actin filaments, as it associates with a preexisting filament to induce the assembly of a branching filament, thus generating dendritic arrays. The Arp2/3 complex needs to be activated by Nucleation Promoting Factors (NPFs). The most potent NPFs contain a C-terminal VCA domain (Verprolin homology or WH2–Connector–Acidic) that binds to both actin and the Arp2/3 complex (Pollard, 2007). VCA domain-containing proteins are divided into four families: WASP, WAVE, WHAMM/JMY, and WASH. Whereas the existence of WASP and WAVE families has been known for a decade, WHAMM/JMY and WASH families were only recently discovered (Campellone et al., 2008; Linardopoulou et al., 2007; Zuchero et al., 2009). A unique amino-terminal domain characterizes each of these families.

The cellular functions of NPFs have been extensively studied (Takenawa and Suetsugu, 2007). WAVE proteins are required for the formation of lamellipodia and membrane ruffles. WASP proteins are required for the formation of podosomes and for the internalization step of endocytosis. Importantly, WASP proteins were also found to propel endosomes in the cytoplasm under certain conditions (Benesch et al., 2002 and references therein). WHAMM is required to maintain Golgi morphology and to facilitate transport along the biosynthetic pathway (Campellone et al., 2008). JMY, despite significant homologies to WHAMM, regulates transcription and cell migration (Zuchero et al., 2009).

WASH is an NPF in vitro, but its role in vivo is unclear. The WASH family comprises a single gene in *Drosophila*, *Caenorhabditis elegans*, and mouse genomes, but several paralogous genes in the human genome (Linardopoulou et al., 2007). The WASH gene is essential in *Drosophila*, where it controls morphogenesis of the egg chamber (Linardopoulou et al., 2007; Liu et al., 2009). Here, we characterized the role and the regulation of mammalian WASH with a focus on the single mouse protein. We uncovered that WASH nucleates actin on endosomes, and that this branched actin network plays an essential role in controlling fission of these organelles. Moreover, we report the existence of a multiprotein complex containing WASH, which is likely conserved in species possessing WASH proteins.

RESULTS

WASH Localizes to a Restricted Domain of Sorting and Recycling Endosomes

We first examined WASH expression and localization by using a polyclonal antibody we generated against the VCA domain. The affinity-purified antibody recognized a major band in 3T3 cell lysate by western blot (see Figure S1A available online). This band was markedly reduced upon siRNA-mediated depletion of WASH (Figure 1A), whereas the amounts of the other NPFs—WHAMM, N-WASP, and WAVE2—were unaffected (Figure S1B). An analysis of several mouse tissues indicated that WASH expression is ubiquitous (Figure 1B; Figure S1C for full

gel). In 3T3 cells, endogenous WASH was localized by immunofluorescence in numerous cytoplasmic spots in the perinuclear region. These spots were reduced in intensity upon WASH depletion, confirming staining specificity (Figure S1D). Because the WASH antibody targets the VCA domain, which is relatively conserved among NPFs, we verified in addition that the WASH antibody does not immunoprecipitate WHAMM, N-WASP, and WAVE2, in conditions under which WASH was fully depleted from the lysate (Figure S1E). To confirm this localization, we generated a stable 3T3 cell line expressing GFP-WASH. The overexpression of GFP-WASH in this line is moderate compared to endogenous WASH in the control line expressing GFP alone (Figure S1F). GFP-WASH expression was accompanied by a downregulation of endogenous WASH, suggesting that GFP-WASH takes the place of endogenous WASH in this cell line. Indeed, the localization of GFP-WASH was the same as endogenous WASH (Figure S1G). A localization in lamellipodia upon transient overexpression of GFP-WASH was previously reported (Linardopoulou et al., 2007), but we found no evidence of endogenous WASH in lamellipodia of several cell lines (data not shown). WASH was consistently present in cytoplasmic spots.

To characterize these spots, we attempted to colocalize them with a series of well-characterized markers. There was no significant colocalization with the *cis*-Golgi marker GM130 (Figure 1C), nor with the *trans*-Golgi network marker TGN38 (Figure 1D). To label sorting and recycling endosomes, cells were loaded until equilibrium with fluorescent transferrin (Tf) (Figure 1E). Colocalization was extensive in this case. Consistently, colocalization was also extensive with EEA1, a marker of sorting endosomes (also known as Early Endosomes) (Figure 1F). In 3T3 cells, sorting endosomes are relatively clustered in the perinuclear region. To examine endosomal compartments involved in the degradative pathway, we labeled lysosomes with Lamp1 (Figure 1G). Colocalization of Lamp1 with WASH was limited to occasional WASH spots on lysosomes.

To confirm these steady-state findings, we performed kinetic analyses of Tf uptake and recycling (Figure S2). The first structures seen, clathrin-coated pits, were devoid of WASH. However, as early as 2 min later, Tf reached sorting endosomes, in which a high level of colocalization with WASH was observed. Importantly, this colocalization was maintained until the Tf signal decreased because of continued recycling. These results confirm that WASH is associated with both sorting and recycling endosomes. We also followed the LDL cargo, which is sorted toward the degradative pathway (Figure S3). After a 10 min pulse incubation, LDL reached sorting endosomes, in which it clearly colocalized with WASH. When LDL was chased, it appeared in larger organelles, lysosomes, most of which were not labeled by WASH antibodies. These kinetic analyses confirmed that WASH localizes to endosomes, with an enrichment in the recycling pathway compared to the degradative pathway.

WASH localization was further characterized by using Rab GTPases, which coordinate trafficking events and can be used as markers of different compartments (Zerial and McBride, 2001). Recycling pathways were followed by using Rab4 and Rab11, markers of fast and slow recycling, respectively. Colocalization between WASH and Rab11 was evaluated by time-lapse imaging, because the GFP-Rab11 signal blurs upon fixation. Consistent with previous results, WASH colocalized with both Rab4 and Rab11, although to a higher extent with Rab4 (Figures 1H and 1I; Movies S1 and S2). Rab5 is enriched in newly internalized vesicles and sorting endosomes, where it regulates fusion events. Colocalization between WASH and Rab5 was significant (Figure 1J; Movie S3), confirming the localization of WASH on sorting endosomes. Finally, we examined Rab7, which is a marker of late endosomes in the degradative pathway. WASH was moderately associated with Rab7 compartments (Figure 1K). Together, these results establish that WASH is localized on different populations of endosomes, with an enrichment in the recycling pathway compared to the degradative pathway. This distribution of WASH in the different endosomal compartments is summarized in Figure 1L.

Interestingly, this colocalization analysis revealed that WASH never fully overlaps with any given marker. Even with Tf, WASH appeared juxtaposed rather than superimposed on Tf spots (inset of Figure 1E), as one would expect if WASH was covering Tf-containing endosomes. To better visualize the two signals, we performed a three-dimensional (3D) reconstruction after sectioning of the cell along the z axis (Figure 2A; Movie S4). This confirmed that WASH and Tf fluorescence centroids were not superimposed. Because WASH spots are localized at different positions on endosomes in a single field, it rules out any aberrant translational shift in the acquisition of the two channels. Dual-color time-lapse imaging further confirmed that the two spots were always associated and thus did not correspond to different organelles only transiently associated (Figure 2B; Movie S5). To further prove this point, centroids of fluorescence were tracked over time, and the distance between them was calculated (Figure 2C; Figure S4 for the analysis of multiple endosomes). This distance fluctuates over time, between 0 and 0.3 μm, which is the apparent radius of the Tf-containing vesicle. Importantly, there was no influence of endosome movement on the fluctuation of this distance. This is a strong argument that WASH has a restricted localization on endosomal membranes. Because the size of endosomes is about the resolution of optical microscopy, we enlarged endosomes by expressing the active form of Rab5, which promotes endosomal fusion (Zerial and McBride, 2001). As expected, WASH staining did not cover the periphery of these enlarged endosomes, but displayed rather discrete spots (Figure 2D). A 3D reconstruction unambiguously established that WASH is present on distinct domains at the surface of these large endosomes (Figure 2E; Movie S6). These enlarged endosomes additionally revealed that the WASH domains were highly dynamic at their surface (Movie S7).

WASH Activates Arp2/3-Mediated Actin Polymerization on Endosomes

F-actin, the Arp2/3 complex, and the marker of branched actin networks, cortactin, were previously detected on endosomes (Kaksonen et al., 2000). However, the NPF responsible is not yet known; thus, we examined whether WASH would polymerize actin on endosomes. The vast majority of WASH spots appeared to be associated with small F-actin structures (Figure 3A). Importantly, in dual-color time-lapse imaging, the association between WASH and F-actin was continuous over time (Movie S8). Consistent with the F-actin staining, most WASH spots also contained the Arp2/3 complex (Figure 3B). However, there were more Arp2/3 spots than WASH spots in the perinuclear region, likely

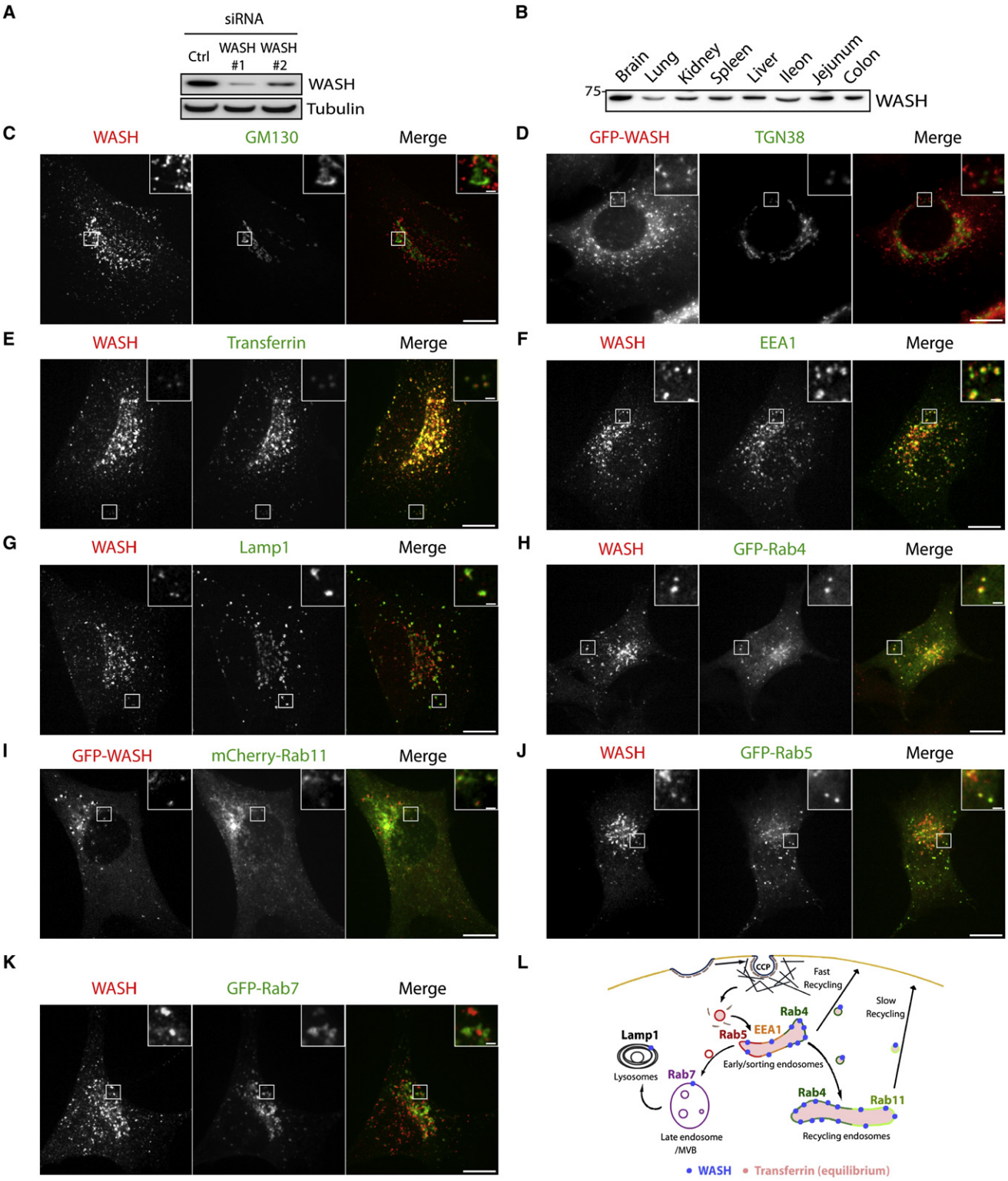

Figure 1. WASH Localizes to Sorting and Recycling Endosomes

(A) Specificity of WASH antibodies is validated by western blot lysates of siRNA-transfected 3T3 cells.

(B) WASH is ubiquitously expressed in mouse tissues.

(C–K) Colocalization of WASH with various endocytic markers. 3T3 cells were processed for immunofluorescence with the indicated antibodies. Rab11-expressing cells were imaged live, and a single image extracted from the movie is shown. A single plane of spinning disk confocal microscopy is shown, except for TGN38 (epifluorescence). A stable 3T3 line expressing GFP-WASH is used when indicated. Fluorescent fusion proteins of Rab 4, 5, 7, and 11

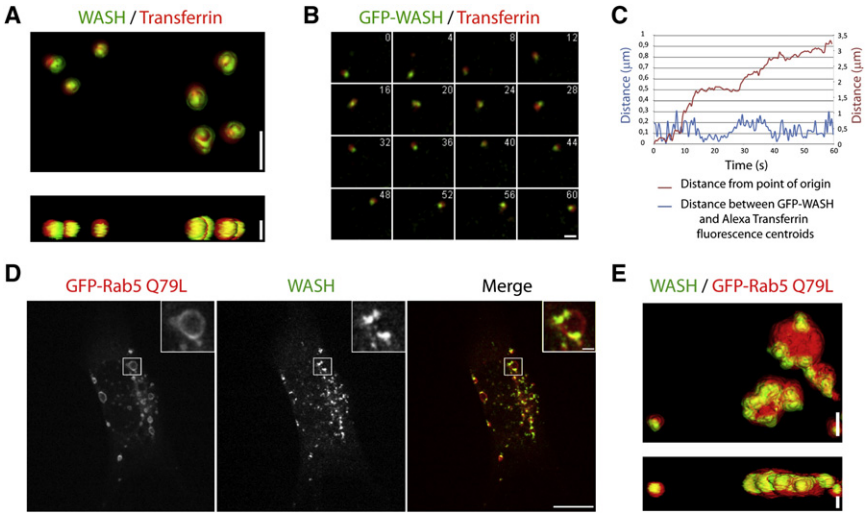

Figure 2. WASH Has a Restricted Localization at the Surface of Endosomes

(A) 3T3 cells were loaded with fluorescent Tf until equilibrium, then processed for immunofluorescence with WASH antibodies. Confocal z sections were acquired and processed for 3D reconstruction. Front and side views are shown. Note the limited overlap between WASH and Tf signals. The scale bar represents 1 μm.

(B) 3T3 cells stably expressing GFP-WASH were loaded with fluorescent Tf until equilibrium, then processed for time-lapse imaging by using spinning disk confocal microscopy. The behavior of a single moving endosome is shown. Elapsed time is in seconds. The scale bar represents 1 μm. WASH and Tf are continuously associated, but do not fully overlap.

(C) Tracking of fluorescence centroids of GFP-WASH and Tf from the endosome displayed in (B) shows that the distance between the two spots is always below the apparent radius of the endosome (0.3 μm), whether or not the endosome moves. The scale bar represents 1 μm.

(D) 3T3 cells were transfected with GFP-Rab5 Q79L to enlarge endosomes and were processed for immunofluorescence with WASH antibodies. Images correspond to a single confocal plane. The scale bar represents 10 μm (1 μm in inserts). WASH localizes to discrete spots at the periphery of the enlarged endosome.

(E) Confocal z sections were acquired on a cell treated as in (D) and processed for 3D reconstruction as in (A). The scale bar represents 1 μm.

because Arp2/3 can be recruited by other NPFs such as WHAMM or N-WASP. Interestingly, WASH was absent from the tip of actin comet tails induced by the overexpression of PIP5-kinase (Movie S9), indicating that WASH is not involved in the so-called "endosomal rocketing," which requires N-WASP (Benesch et al., 2002). Long-range movements of WASH-positive endosomes depended on microtubules (MTs), as revealed by treatment with the MT-depolymerizing drug, nocodazole (Movie S10, to be compared to Movie S5). To prove that WASH was responsible for the actin polymerization on endosomes, transfection of siRNAs was used to deplete WASH from 3T3 cells. Upon WASH depletion, most F-actin spots and a large fraction of Arp2/3 complex spots in the perinuclear region disappeared, indicating that WASH has a major role among the perinuclear NPFs (Figure S5).

The staining of F-actin structures with phalloidin was too crowded to permit an accurate quantification. To quantify Arp2/3 complex and cortactin recruitment on endosomes, we used a mild pre-extraction procedure that allowed us to eliminate specifically the contribution of the cytosolic pool of these proteins (Figure S6A). When cells loaded with fluorescent Tf were examined by immunofluorescence for the localization of the Arp2/3 complex, endosomes were found to associate with the Arp2/3 complex (Figure 3C). Upon WASH depletion, this association was drastically affected (Figure S6 for a second siRNA), even though some perinuclear staining of the Arp2/3 complex was retained, in agreement with the fact that not all perinuclear Arp2/3 complex spots are associated with WASH. Quantifications confirmed that WASH played a major role in recruiting the Arp2/3 complex onto endosomes (Figure 3D). The same analysis conducted on cortactin recruitment gave similar results (Figures 3E and 3F). To confirm the specificity of this phenotype, we decided to perform rescue experiments in the stable 3T3 cell line expressing GFP-WASH, since transient overexpression of WASH has deleterious effects on Arp2/3-dependent structures (Figure S7B). GFP- or GFP-WASH-expressing cell lines were transfected with a WASH siRNA that recognizes the 3′UTR of WASH, which is absent from the GFP-WASH mRNA. Indeed, endogenous WASH was depleted from GFP-expressing cells, but GFP-WASH was not depleted from GFP-WASH-expressing cells (Figure S7C). Importantly, WASH siRNA transfection induces a loss of Arp2/3 complex (Figure 3G) and cortactin (Figure 3H) recruitment on endosomes in the GFP cell line, but not in the GFP-WASH cell line. This result not only establishes that the lack of Arp2/3 complex and cortactin recruitment on endosomes obtained upon siRNA-mediated depletion of WASH can be rescued, but it also validates that the GFP-WASH fusion protein used in this study is a functional WASH protein.

This set of experiments demonstrates that WASH is an active NPF at the surface of endosomes, where it recruits and activates the Arp2/3 complex to induce actin polymerization.

WASH Is Part of a Large Multiprotein Complex Containing CP

An important level of regulation of NPFs is their inclusion in stable multiprotein complexes. N-WASP is associated with WASP-interacting protein (WIP) family proteins, and the WAVE proteins are incorporated into a large complex of five subunits (Takenawa and Suetsugu, 2007). To examine whether WASH is included in

were transiently transfected. When indicated, 3T3 cells were loaded with fluorescent Tf until equilibrium. The scale bars in (C–K) represent 10 μm (1 μm in inserts).

(L) Scheme recapitulating the localization of WASH in the different compartments. CCP, clathrin-coated pit; MVB, multivesicular bodies.

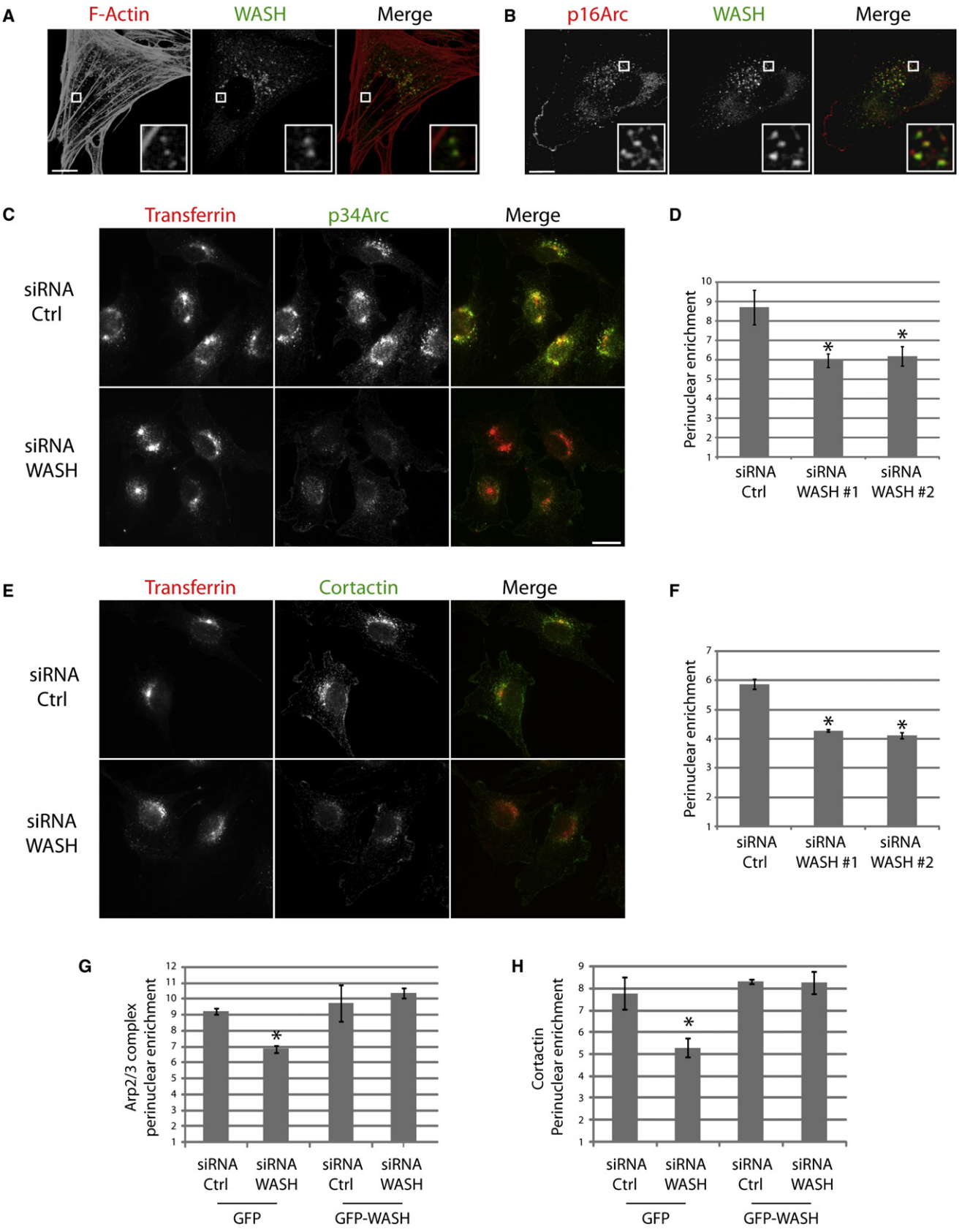
A
F-Actin
WASH
Merge
B
p16Arc
WASH
Merge
C
Transferrin
p34Arc
Merge
siRNA Ctrl
siRNA WASH
D
Perinuclear enrichment
siRNA Ctrl
siRNA WASH #1
siRNA WASH #2
E
Transferrin
Cortactin
Merge
siRNA Ctrl
siRNA WASH
F
Perinuclear enrichment
siRNA Ctrl
siRNA WASH #1
siRNA WASH #2
G
Arp2/3 complex perinuclear enrichment
siRNA Ctrl
siRNA WASH
siRNA Ctrl
siRNA WASH
GFP
GFP-WASH
H
Cortactin Perinuclear enrichment
siRNA Ctrl
siRNA WASH
siRNA Ctrl
siRNA WASH
GFP
GFP-WASH

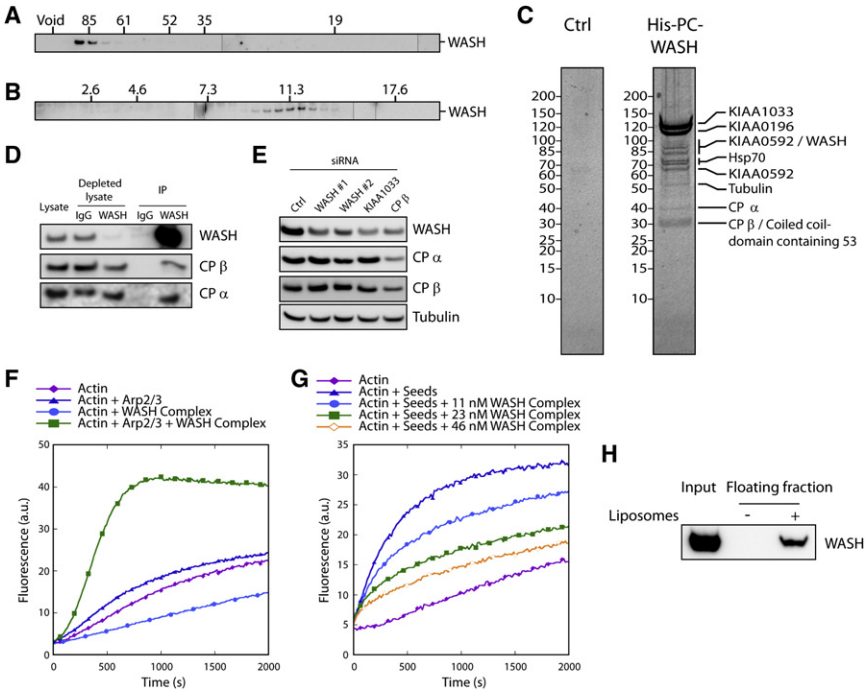

Figure 4. A Multiprotein Complex Containing WASH and Capping Protein Binds to Liposomes and Activates Actin Polymerization In vitro

(A and B) WASH belongs to a high-molecular weight complex. (A) Size-exclusion chromatography of a 3T3 cell lysate. Elution fractions were analyzed by WASH western blot (WB). The Stokes' radius of standards is given in Å. (B) Ultracentrifugation of a 3T3 cell lysate in a sucrose gradient. Fractions were analyzed by WASH WB. The sedimentation coefficient of standards is given in Svedberg (S).

(C) Identification of the WASH complex. 293 cells stably expressing His-PC-WASH or the empty plasmid were lysed and submitted to two steps of affinity chromatography. WASH and its associated proteins were stained by Coomassie blue and identified by mass spectrometry. Molecular weight markers in kDa are indicated on the left of each gel.

(D) CP is a bona fide component of the WASH complex. Lysates from 3T3 cells were analyzed by immunoprecipitation with WASH antibodies or nonimmune IgG. Lysates and immunoprecipitates were analyzed by WB with the indicated antibodies. A pool of the CP belongs to the WASH complex.

(E) Depletion of WASH complex subunits downregulates the WASH protein. 3T3 cells were depleted of KIAA1033, CP β, or WASH by using siRNAs. Amounts of these proteins in total cell lysates were analyzed by WB.

(F) The WASH complex activates Arp2/3-mediated actin nucleation. Conditions: 2.5 μM actin (10% pyrene labeled), 20 nM Arp2/3 complex, and 35 nM WASH complex.

(G) The WASH complex blocks elongation of barbed ends, indicating that the CP contained within the complex is not fully masked. Unlabeled F-actin seeds (1 μM) and the WASH complex were preincubated before addition of G-actin (1.5 μM, 10% pyrene labeled) and initiation of actin polymerization.

(H) The WASH complex binds directly to liposomes. When liposomes made of purified brain lipids, mixed with purified WASH complex, were floated on a sucrose cushion, WASH was brought in the floating fraction, as revealed by WB.

a multiprotein complex, we first estimated its apparent molecular weight by using size-exclusion chromatography. A detergent extract was prepared from 3T3 cells and loaded on a superdex-200 column. A single peak of WASH was detected after the void volume and before the largest marker (thyroglobulin, 669 kDa, 85 Å; Figure 4A). The Stokes' radius of native WASH was estimated at 88 Å. We complemented this analysis by ultracentrifugation. The detergent extract was loaded on top of a linear sucrose gradient. A single peak of WASH was detected (Figure 4B). WASH sedimented faster than the catalase marker (232 kDa, 11.3 S). The sedimentation coefficient of WASH was estimated at 12.5 S. These values of Stokes' radius and sedimentation coefficient correspond to a molecular weight of ~450 kDa (see Supplemental Data). Because WASH is ~50 kDa, these experiments indicate that WASH is included in a single complex of high molecular weight.

To purify the WASH complex, we selected a stable 293 human cell line expressing WASH dually tagged with $(His)_6$ and Protein C

Figure 3. WASH Is Required for Arp2/3-Mediated Actin Polymerization on Endosomes

(A and B) WASH is associated with perinuclear structures containing F-actin and the Arp2/3 complex. 3T3 cells were processed for immunofluorescence with WASH antibodies and either (A) fluorescent phalloidin to stain F-actin structures or an (B) antibody recognizing the p16Arc subunit of the Arp2/3 complex. Each image corresponds to a single confocal plane. The scale bar represents 10 μm.

(C) WASH is required for recruitment of the Arp2/3 complex on endosomes. Transfected cells were loaded with fluorescent Tf. Cells were then pre-extracted and processed for immunofluorescence with an antibody recognizing the p34Arc subunit of the Arp2/3 complex. Recruitment of the Arp2/3 complex on endosomes is greatly decreased in WASH-depleted cells. The scale bar represents 10 μm.

(D) Quantification of Arp2/3 complex enrichment on perinuclear endosomes in cells treated as in (C). A perinuclear region of interest is defined by thresholding the Tf signal. This region of interest is then shifted to another region of the cytoplasm. In these two regions with the same area, p34Arc intensities are integrated. Perinuclear enrichment refers to the ratio of these two values. Mean ± standard error of the mean (SEM) of this ratio is plotted (three independent experiments, $n > 60$ cells in each condition, $^*p < 0.001$ compared with the control).

(E) WASH is required for recruitment of cortactin on endosomes. Cells treated as in (C) were processed for immunofluorescence with a cortactin antibody.

(F) Quantification of cortactin enrichment on perinuclear endosomes in cells treated as described in (E). Quantification as in (D) (three independent experiments, $n > 50$ cells in each condition, $^*p < 0.001$ compared with the control).

(G and H) Rescue of the recruitment of Arp2/3 and cortactin on endosomes by GFP-WASH expression. Stable 3T3 cell lines expressing either GFP or GFP-WASH were treated and processed as in (C) and (E). GFP-WASH is resistant to the WASH siRNA that targets a region of the 3′UTR, which is absent from the GFP-WASH construct. Arp2/3 (respectively Cortactin) recruitment on Tf-containing endosomes was quantified as in (D) and (F) (mean ± SEM, three independent experiments, $n > 40$ cells in each condition, $^*p < 0.001$ compared with the control).

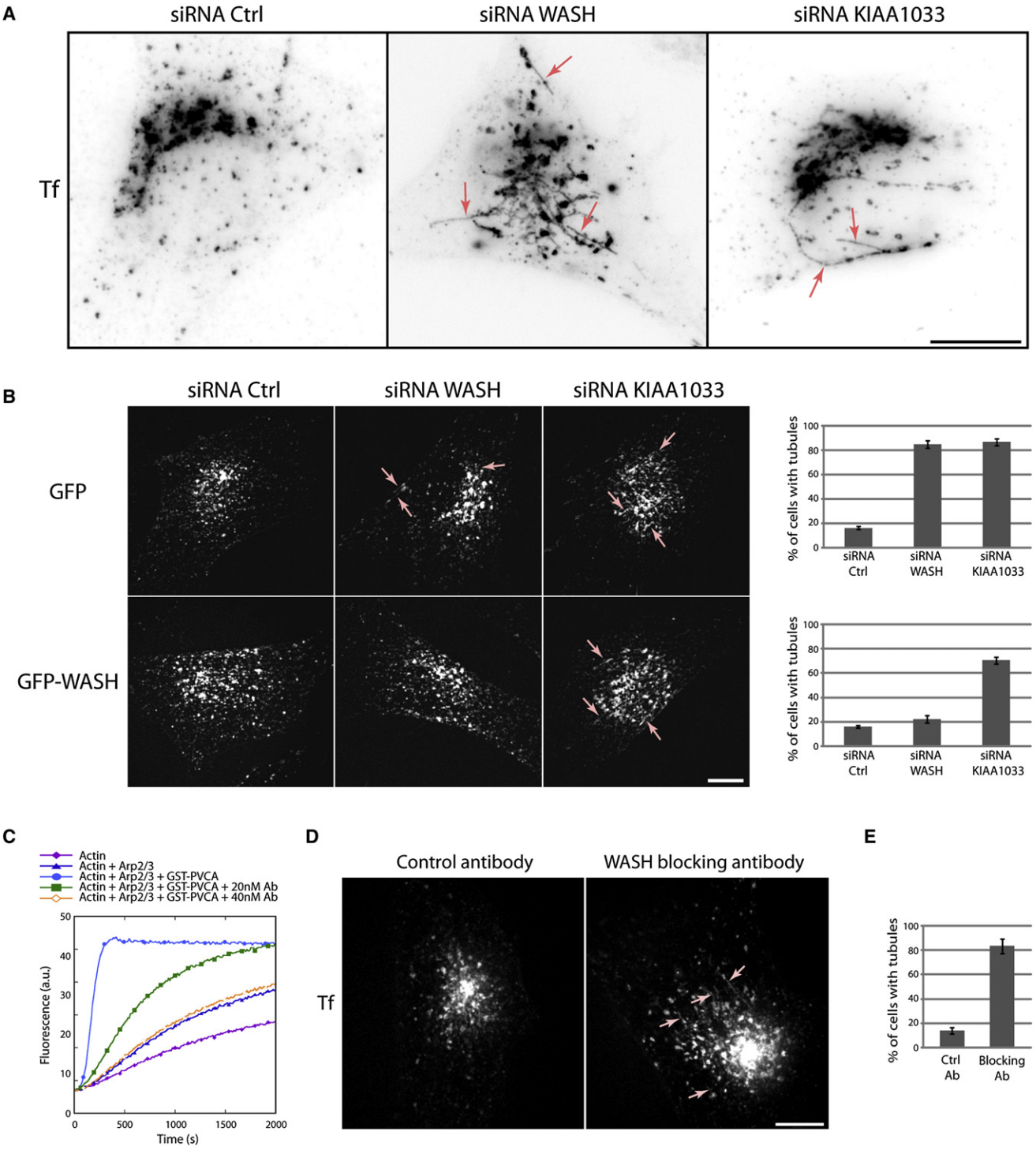

Figure 5. WASH Inhibition Induces Tubulation of Endosomes

(A) WASH was depleted from 3T3 cells by using siRNAs targeting either WASH itself or the KIAA1033 subunit. Cells were loaded with fluorescent Tf until equilibrium, then fixed and observed by epifluorescence microscopy. Numerous long and narrow tubules containing Tf are observed upon WASH depletion (arrows). The scale bar represents 10 μm.

(B) Rescue of the tubulation phenotype by GFP-WASH expression. Stable 3T3 cell lines expressing either GFP or GFP-WASH were treated with the same siRNAs as in (A). GFP-WASH is resistant to the WASH siRNA that targets the 3′UTR. Cells were imaged by time-lapse spinning disk confocal microscopy in the presence of fluorescent Tf. A single image from the movies is extracted. Arrows indicate tubulated endosomes. siRNA targeting WASH induces tubulation of the GFP cell line, but not of the GFP-WASH cell line, indicating that the tubulation phenotype is specifically due to WASH targeting, and not to an off target. Cells displaying tubules were counted live on the criterion that they exhibited at least one tubule stable for at least 5 s (mean ± SD of two independent experiments, n > 82 cells for each condition). The scale bar represents 10 μm.

(PC) tags. We then used a Tandem Affinity Purification (TAP) protocol to purify WASH. Upon Coomassie staining, numerous proteins appeared to be associated with WASH, whereas the same experiment conducted with a control line gave no detectable protein (Figure 4C). These proteins were identified by LC-MS/MS (Table S1). Three uncharacterized proteins of high molecular weight, KIAA1033, KIAA0196, and KIAA0592, were associated with WASH. Some Hsp70 proteins were identified, indicating that part of the purified WASH proteins were still in the process of folding. Tubulin was also found to associate with WASH. The two subunits of Capping Protein (CP), α and β, together with the uncharacterized "coiled-coil domain containing 53" protein that comigrates with CP β are WASH partners of lower molecular weight. If the Hsp70 proteins and tubulin are excluded, which are abundant proteins and likely transient interactors, a potential multiprotein complex of seven subunits—KIAA1033, KIAA0196, KIAA0592, WASH, CP α, CP β, and "coiled-coil domain containing 53"—remains. Upon summing the mass of each of these subunits, we obtain a mass of 550 kDa, in relative agreement with the characterization of native WASH given the uncertainty of the Stokes' radius measurement above the last marker. Because a stoichiometry of one subunit per complex already gives a larger complex than measured, it is likely that we have identified the entire WASH complex.

The presence of CP in the WASH complex was particularly intriguing, because CP is known to exist as a free heterodimer (Cooper and Sept, 2008). To confirm the association of CP with endogenous WASH, we immunoprecipitated WASH efficiently so as to deplete the cell lysate (Figure 4D). The immunoprecipitate contained a pool of both CP α and β. We also found that CP β colocalizes with WASH continuously over time in the perinuclear region (Movie S11). CP β was also found in lamellipodial/ruffling regions of the plasma membrane without WASH, as expected. The WASH immunoprecipitation and the imaging confirmed that at least two distinct pools of CP exist in the cell. A general property of stable multiprotein complexes is that some subunits depend on others for their stability, a phenomenon well described for the WAVE complex (Takenawa and Suetsugu, 2007). We found that WASH was as deeply downregulated in 3T3 cells when KIAA1033 or CP β was targeted as when WASH itself was targeted (Figure 4E). We extended this result in HeLa cells. Transfection of shRNA-encoding plasmids targeting any of the seven proposed subunits destabilized the WASH protein (Figure S8), confirming that these seven proteins are part of the same stable multiprotein complex.

CP inhibits actin dynamics at the barbed end of the filament. It is thus an activity that can oppose the generation of new barbed ends by the active Arp2/3 complex. We tested whether the purified WASH complex was able to promote actin polymerization in vitro. We first verified that WASH constructs containing the VCA domain were able to activate Arp2/3-dependent actin polymerization in vitro by inducing branches (Figure S9). When the purified WASH complex was assayed in vitro, it was found to enhance the basal Arp2/3 complex activity (Figure 4F), in line with the fact that most WASH spots were associated with F-actin in vivo. However, the WASH complex in absence of the Arp2/3 complex slowed down the kinetics of spontaneous actin polymerization (Figure 4F). This effect might be due to sequestration of G-actin by the WH2 domain present in the WASH VCA domain or to the capping activity of CP present in the complex. We ruled out the possibility that this effect might be due to the WH2 domain, because VCA at the same concentration does not display this inhibitory effect (Figure S10B). To directly check whether CP within the WASH complex was active, we specifically monitored elongation at barbed ends by including F-actin seeds. The WASH complex exerted a dose-dependent inhibitory effect (Figure 4G). However, this effect was observed at much higher concentrations than the inhibitory effect obtained with the free heterodimer of CP (Figure S10), indicating that the binding constants of CP to F-actin were significantly affected by its inclusion into the WASH complex. Thus, the WASH complex promotes efficient actin nucleation by the Arp2/3 complex, despite partial activity of its CP component.

We then tested whether the purified WASH complex was able to directly interact with lipids. For this purpose, we generated liposomes from purified bovine brain lipids. When these liposomes were floated on a sucrose cushion by ultracentrifugation, they carried interacting proteins such as the protein IRSp53, containing a RCB/IMD domain (Takenawa and Suetsugu, 2007), but not GST (Figure S11). When these liposomes were mixed with the WASH complex, WASH was detected in the top fraction (Figure 4H). These results indicate that the restricted localization of WASH on endosomal membranes might be due, at least in part, to a direct interaction of the WASH complex with endosomal lipids.

WASH Inactivation Induces Endosome Tubulation

Actin polymerization by the Arp2/3 complex is known to generate a force that pushes or remodels membranes (Takenawa and Suetsugu, 2007). We thus decided to investigate the morphology of endosomes upon WASH inactivation. Fluorescent Tf was loaded until equilibrium in 3T3 cells previously transfected with siRNAs targeting WASH or KIAA1033. Cells depleted of CP β were not analyzed further, because the free pool of CP was depleted together with WASH in this case. Strikingly, in WASH-depleted cells, long and narrow tubules containing Tf were observed (Figure 5A). These tubules were up to 10 μm long and originated from larger round endosomes. Such long tubules were never observed in control cells. We thus sought to confirm these findings by live cell imaging of fluorescent Tf. Indeed, 3T3 cells treated with control siRNAs do not display Tf-positive tubules (Movie S12), whereas many of these were present in WASH-depleted cells (Movie S13). The compartments labeled with the Rab GTPases that colocalized with WASH,

(C) The antibody targeting the VCA domain of WASH blocks the NPF activity of WASH in vitro. Conditions: 2.5 μM actin (10% pyrene labeled), 25 nM Arp2/3 complex, and 62.5 nM GST-PVCA.

(D) Microinjection of the WASH antibody induces the tubulation of endosomes. 3T3 cells were microinjected with WASH or control antibodies, loaded with fluorescent Tf until equilibrium, and imaged by time-lapse spinning disk confocal microscopy. The scale bar represents 10 μm.

(E) Quantification as in (B) of the effect seen in (D) (mean ± SD of three independent experiments, n > 12 cells for each condition in duplicate). The difference is statistically relevant ($p < 0.001$, Student's t test).

Rab4, Rab5, Rab7, and Rab11 were all tubulated upon WASH depletion (Figure S12), indicating that this phenotype is not restricted to a subpopulation of endosomes. Time-lapse imaging revealed that Tf-containing tubules were highly dynamic. In many instances, a tubule elongates and the endosome follows on the same track (Figure S13A), suggesting that both endosome tubulation and movement depend on MT and MT motors. Indeed, MT depolymerization with nocodazole prevented endosome tubulation (Figure S13B).

To confirm the specificity of this phenotype, we performed rescue experiments in the stable 3T3 cell lines expressing GFP or GFP-WASH as before. siRNA-transfected cells were then loaded with fluorescent Tf and imaged live by using spinning disk confocal microscopy (Movie S14). Importantly, upon WASH siRNA transfection, many Tf-containing tubules were observed in the GFP cell line, but not in the GFP-WASH cell line (Figure 5B). In addition, transfection of KIAA1033 siRNA induced tubules in both cell lines, indicating that the GFP-WASH-expressing cell line was able to form endosome tubules if the WASH complex was targeted. Tubulation was quantified from real time observation of cells. The reported effects were highly reproducible in two independent experiments. Thus, tubulation of endosomes is specifically associated with the depletion of the WASH complex. However, this complex might have other important functions in addition to polymerizing actin at the surface of endosomes. In order to specifically affect actin polymerization at the surface of endosomes, we utilized the WASH antibody that targets its VCA domain. In pyrene-actin assays, this WASH antibody blocked the ability of WASH fusion proteins containing the VCA domain to activate Arp2/3-mediated nucleation, but did not affect the VCA domains from WAVE2 or N-WASP (Figure 5C; Figure S14A). It also efficiently blocked the activity of the WASH complex toward the Arp2/3 complex (Figure S14B). When microinjected into cells, this antibody induced tubulation of Tf-containing endosomes (Figure 5D; Movie S15, quantification in Figure 5E). Thus, the WASH complex and specifically its ability to activate the Arp2/3 complex are required to maintain the morphology of endosomes and to prevent them from tubulating.

To examine the physiological consequence on trafficking, we turned to well-established assays of Tf recycling in HeLa cells. When Tf internalization was monitored by flow cytometry, WASH-depleted cells contained a higher amount of Tf at all time points (Figure 6A), suggesting that either internalization was increased or recycling was impaired. Given the extensive colocalization of WASH with internal endosomes, we tested specifically whether Tf recycling was affected. We loaded cells with fluorescent Tf and examined the rate of its release. At all time points examined, WASH-depleted cells contained a higher amount of Tf (Figure 6B), indicating that, indeed, Tf recycling is impaired in WASH-depleted cells.

Endosomes are sorting platforms for cargoes taking different routes. This sorting is mediated by vesicular or small tubular transport intermediates (Maxfield and McGraw, 2004). The long tubules and the defect in Tf recycling observed in WASH-depleted cells could be the consequence of a defective fission of transport intermediates. One of the best characterized machineries performing membrane fission is the GTPase dynamin, which can be specifically inhibited by dynasore. We loaded cells with fluorescent Tf and examined the Tf compartment upon dynasore treatment. Dynasore induced tubulation of endosomes, like WASH depletion (Figure 6C). As in WASH-depleted cells, the compartments labeled with Rab4, Rab5, Rab7, and Rab11 were tubulated upon inhibition of dynamin (Figure S12). Dynasore-induced tubules aligned with MT tracks, as expected (Figure S13C). Importantly, WASH was detected at the level of mother endosomes, but never along the dynasore-induced tubules emerging from them (Figure 6D; Movie S16). This similar phenotype upon WASH inactivation and dynamin inhibition prompted us to examine whether WASH interacts with dynamin. Indeed, immunoprecipitation of endogenous WASH revealed associated endogenous dynamin (Figure 6E). The reverse coimmunoprecipitation was attempted with wild-type (WT) and the inactive K44A mutant of dynamin. WT and mutant dynamin associated to the same extent with endogenous WASH, indicating that the interaction of WASH with dynamin is not regulated by the activity of the latter (Figure 6F). Together, these results suggest that dynamin may play a role downstream of WASH in the fission of transport intermediates from endosomes, in line with a defective recruitment and/or activation of dynamin when WASH is inactivated, giving rise to endosome tubulation.

DISCUSSION

WASH belongs to a multiprotein complex, as has been demonstrated for other well-characterized NPFs. This complex that we have purified contains seven subunits, and it is likely to be a stable multiprotein complex, i.e., a molecular machine, because we have obtained evidence that WASH depends on other subunits for its stability. The WASH complex appears to be constitutively active in its ability to promote Arp2/3-dependent nucleation, in contrast to the WAVE complex, which is intrinsically inactive (Derivery et al., 2009). The identification of CP in the WASH complex was a surprise. CP is already a complex, a heterodimer, that is incorporated into a ''supercomplex.'' It has previously been shown that the heterodimer of CP is part of the Dynactin complex, which contains a minifilament of actin-related proteins (Schroer, 2004). However, the WASH complex contains both an NPF and a CP, which is known to inhibit actin dynamics at the barbed end of filaments (Cooper and Sept, 2008), and thus represents a potential antagonist of the NPF.

CP has long been recognized as an essential component of force generation by Arp2/3-mediated branched actin networks in vitro (Loisel et al., 1999) and in vivo (Mejillano et al., 2004). Without CP, all filaments in the network can be elongated, generating a ''fishbone'' appearance of comet tails obtained in biomimetic assays (Pantaloni et al., 2000). Recent evidence indicated that CP is more tightly associated with the generation of new actin filaments than suspected, because CP promotes Arp2/3-mediated nucleation in vitro (Akin and Mullins, 2008). This role is in line with in vivo observation that CP is enriched at the tip of lamellipodia, where the WAVE NPF is active (Lai et al., 2008; Mejillano et al., 2004), rather than having a homogeneous distribution across the lamellipodia as initially thought. We were able to detect low but significant CP activity within the purified WASH complex. This CP activity might also promote Arp2/3 activation, as proposed for the free heterodimer of CP (Akin and Mullins, 2008). CP and WASH activities might also be sequentially revealed in a molecular cycle of activation. For example,

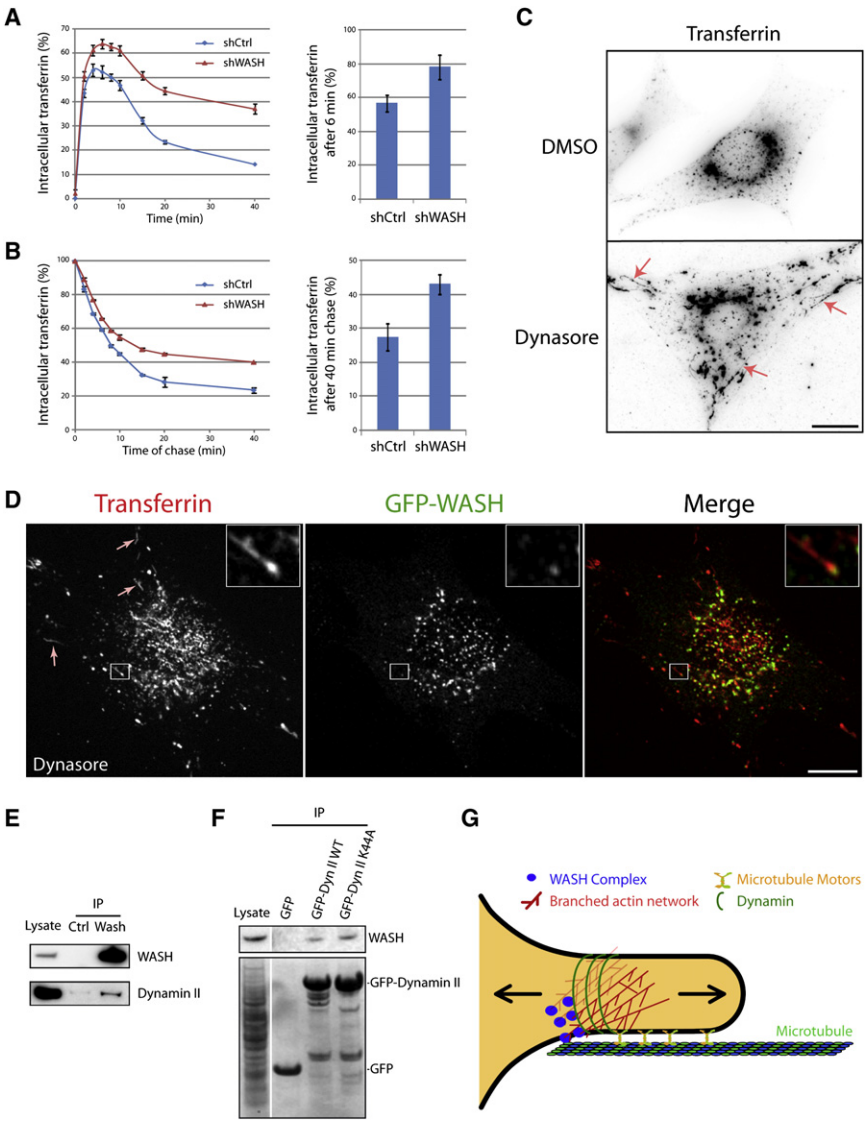

Figure 6. WASH Controls the Fission of Transport Intermediates through an Interaction with Dynamin

(A) HeLa cells transfected with WASH targeting shRNA or control shRNA were incubated with fluorescent Tf at 4°C. After a shift to 37°C for the indicated times, cells were acid washed to remove membrane Tf. Intracellular Tf was then quantified by flow cytometry. Intracellular Tf is expressed as a percentage of prebound Tf. A single representative experiment with duplicate measurements is plotted (mean ± SD). The histogram shows the mean ± SD of three independent experiments. WASH-depleted cells internalize a higher amount of Tf, suggesting that either uptake or recycling to the plasma membrane is affected.

(B) Similarly transfected HeLa cells were loaded with fluorescent Tf for 6 min at 37°C as in (A) and then acid washed at 4°C. After a shift to 37°C for the indicated times, intracellular Tf was quantified by flow cytometry. Intracellular Tf is expressed as a percentage of the initial intracellular Tf. A single representative experiment with duplicate measurements is plotted (mean ± SD). The histogram shows the mean ± SD of two independent experiments. WASH-depleted cells are slower to release internal Tf, indicating that its recycling to the plasma membrane is affected.

(C) Pharmacological inhibition of dynamin mimics WASH depletion. 3T3 cells were loaded with fluorescent Tf until equilibrium, then dynasore (80 μM) was added in the presence of Tf for 30 min. Cells were processed as in Figure 5A. Numerous long and narrow tubules containing Tf are observed (arrows). The scale bars represents 10 μm.

(D) 3T3 cells expressing GFP-WASH treated with dynasore as in (C) were imaged by time-lapse spinning disk confocal microscopy. A single image is extracted from the movie. GFP-WASH does not localize along the tubules, but to the mother endosomes. The scale bars represents 10 μm.

(E) WASH and dynamin II coprecipitate. WASH was immunoprecipitated from a lysate of B16F1 cells. The immunoprecipitates were analyzed with WASH or dynamin II antibodies.

(F) The interaction of dynamin with WASH does not depend on its activity. 293T cells were transiently transfected with plasmids expressing GFP, GFP-dynamin II WT, or its inactive K44A derivative. GFP fusion proteins were precipitated with GFP-trap resin. The upper panel presents the WASH immunoblot, and the lower panel presents Ponceau staining.

(G) A model for WASH function in endosome fission. A sorting or recycling endosome in the process of budding an intermediate of transport is represented. The WASH complex initiates Arp2/3-dependent actin polymerization and generates a branched actin network on a restricted domain of the endosome. How microtubules are recruited to this domain is not known. The affinity of the WASH complex for tubulin might play a role in this capture, and/or molecular motors at the surface of the endosomes might become clustered by the branched actin network. Eventually, molecular motors in this area bind MTs and begin to pull out a membrane tube. Dynamin interacts with the WASH complex and/or other components of the branched actin network like cortactin, and polymerizes in spirals around the nascent tube. The tension of the membrane is generated by the two opposing forces generated by MT motors pulling on the tube and the branched actin networks pushing on the endosome. This tension facilitates fission by dynamin. If WASH is absent, fission is defective and MT motors pull a long tube of membrane out of the endosome.

the low CP activity might be sufficient to target the WASH complex to pre-existing barbed ends, so that Arp2/3 activation takes place in close proximity to the barbed end of an actin filament, hence generating dense branched actin networks. The identification of the WASH complex opens up exciting future investigations on the structural coordination between CP and the NPF, on the particular architecture of branched actin networks resulting from this coordination, and the generation of force at the level of endosomes.

WASH and WHAMM are two NPFs that function at the surface of internal membranes and endosomes and Golgi, respectively. They also share the property of coordinating the actin and MT cytoskeletons in the formation of membrane tubules, because both WASH and WHAMM interact with tubulin. However, there is a significant difference between these two NPFs. Notably, depletion of WASH induces tubulation, whereas overexpression of WHAMM induces tubulation (Campellone et al., 2008). Consistently, the actin network polymerized by the VCA domain

of WHAMM and the direct interaction of its coiled-coil domain with MTs appear to facilitate the elongation of membrane tubules along MT tracks. In the case of WASH, the interaction we found with tubulin cannot play a role in the tubulation phenotype, because tubules are elongated along MT tracks when WASH is missing. This argues for a critical role of molecular motors in the generation of membrane tubules upon WASH inactivation.

Among the genes encoding subunits of the WASH complex, the gene encoding KIAA0196 (SPG8) has been recently reported to be mutated in Hereditary Spastic Paraplegia (HSP) (Valdmanis et al., 2007). Many genes responsible for HSP are involved in membrane traffic and the MT cytoskeleton (Fink, 2006). Spastin (SPG4), a MT-destabilizing protein that interacts with endosomal ESCRT complex components; the kinesin motor KIF5A (SPG10), which moves intracellular organelles; Spartin (SPG20), which regulates EGF receptor trafficking; ZFYVE27 (SPG33), which interacts with Rab11; and WASH might outline a trafficking pathway essential to preserve motor neurons from degeneration. It will be interesting to examine the genes encoding the other subunits of the WASH complex in families affected by HSP, but in which the disease cannot be ascribed to already identified HSP genes.

The role we propose for WASH in mediating the fission of transport intermediates from sorting and recycling endosomes generalizes the role proposed for N-WASP in facilitating fission from the plasma membrane. N-WASP-mediated actin polymerization is required for the internalization of clathrin-coated pits, which occurs shortly after a burst of actin polymerization (Takenawa and Suetsugu, 2007). Actin polymerization mediated by N-WASP is required for dynamin-mediated fission of tubules induced by the overexpression of F-BAR/EFC proteins (Itoh et al., 2005; Tsujita et al., 2006). Importantly, the native complex of N-WASP with WIP is absolutely required for the physiological regulation of N-WASP by F-BAR/EFC proteins (Takano et al., 2008). This is similar to the requirement of the WASH complex in mediating the fission of transport intermediates from sorting and recycling endosomes.

An important difference with fission from the plasma membrane is that fission at endosomes is likely to involve molecular motors moving along MT tracks. MT motors generate a pulling force on the membrane. The WASH-Arp2/3 pathway controlling actin polymerization generates a pushing force on the endosome. These two opposing forces are likely to increase the tension of the membrane that will undergo fission (Figure 6G). Tension of the membrane facilitates dynamin-mediated fission (Roux et al., 2006). Moreover, MT-dependent pulling forces, as well as actin-dependent pushing forces, have been shown to generate lipid sorting, which might have a contribution of its own in fission (Liu and Fletcher, 2006; Liu et al., 2006; Roux et al., 2005). Such a membrane of altered lipid composition and maintained under tension would be the perfect substrate for dynamin to mediate fission.

EXPERIMENTAL PROCEDURES

Information on cells, plasmids, siRNA sequences, antibodies, and additional procedures are included in the Supplemental Experimental Procedures.

Immunocytochemistry and Time-Lapse Imaging

3T3 cells were plated for 2 hr onto glass coverslips coated with 50 μg/ml fibronectin (Sigma) before each experiment. For immunocytochemistry, cells were fixed in 3% paraformaldehyde, permeabilized in PBS containing 0.05% saponin, then processed for indirect immunofluorescence by using standard techniques. Fixed cells were imaged by epifluorescence microscopy on a Leica DM6000B microscope equipped with a 100× NA 1.4 oil immersion objective and a CoolSnap HQ camera (Photometrics). Confocal optical sections were acquired with a custom spinning disc confocal microscope based on a Nikon TE2000-U inverted microscope, a 100× NA 1.45 oil immersion objective, a Yokogawa CSU22 spinning disk head, and a CoolSnap HQ2 camera (Photometrics) with a binning set to 1 and operated with Metamorph 7.1.4. This microscope was equipped with a temperature control chamber, The Cube (Life Imaging Services). For Figures 3A and 3B, optical sections were acquired with a Leica TCS SP2 confocal microscope equiped with a 100× NA 1.4 oil immersion objective. For time-lapse microscopy, cells were plated onto fibronectin-coated glass plates (IWAKI), cultured for 2 hr at 37°C in DMEM medium without phenol red supplemented with 25 mM HEPES (Invitrogen). Binning was set to 2 in this case, and channels were acquired sequentially. To compensate for the exit of vesicles from the confocal plane, several planes were acquired for each time point and a maximum intensity z projection was calculated.

Image Analysis

Analyses of images and movies were performed with Metamorph, ImageJ (http://rsb.ingo.nih.gov/ij/) and Adobe Premiere softwares. The background of images was homogenously substracted, and gamma settings were not adjusted. For 3D reconstructions, confocal z sections were performed with an increment of 0.2 μm, and images were processed with the VolumeJ plugin of ImageJ (Abramoff and Viergever, 2002). For visualization purposes, diffraction, which artificially elongates round vesicles along the z axis, was corrected by modifying the aspect ratio parameter of VolumeJ from (x,y,z) = (1,1,1) to (x,y,z) = (1,1,0.5). GFP-WASH and Tf were tracked over time by using ImageJ plugin MtrackJ created by Eric Meijering. The perinuclear enrichments of the Arp2/3 complex and cortactin were analyzed after a square root transformation using a two-way ANOVA with treatments and independent experiments as parameters (SigmaStat). The pairwise comparisons were performed with the Tukey Test using an α factor of 0.05.

Purification of the WASH Complex

The WASH complex was essentially purified like the WAVE complex (Derivery et al., 2009), with the following modifications. A total of 5×10^9 cells expressing $(His)_6$-PC-TEV-WASH (3 L of culture, about 10 ml cell pellet) were lysed in 40 ml of 50 mM HEPES, 200 mM NaCl, 1mM $CaCl_2$, 1% Triton X-100, 5% glycerol, 5 mM $MgCl_2$ (pH 7.4). Lysate was incubated with 1 ml of PC beads (Roche) for 4 hr with recirculation at 4°C. PC beads were washed extensively with 50 ml lysis buffer; 50 ml of 50 mM HEPES, 200 mM NaCl, 1 mM $CaCl_2$, 0.4 M sucrose (pH 7.4); 50 ml of 50 mM HEPES, 200 mM NaCl, 0.4 M sucrose (pH 7.4). Elution was then performed in 50 mM HEPES, 200 mM NaCl, 5 mM EGTA, 0.4 M sucrose (pH 7.4). Elution fractions were pooled and dialyzed against 50 mM HEPES, 200 mM NaCl, 10 mM imidazole, 0.4 M sucrose, 1 mM DTT (pH 7.4) overnight. Eluate was then incubated with 50 μl Ni Sepharose High Performance (GE Healthcare) for 3 hr at 4°C. Beads were then washed extensively with 50 mM HEPES, 200 mM NaCl, 10 mM imidazole, 0.4 M sucrose, 1 mM DTT (pH 7.4) and analyzed by SDS-PAGE. LC-MS/MS was performed as described (Derivery et al., 2009). For activity assays, the WASH complex eluted after Protein C affinity column was concentrated by using Amicon Ultra (Millipore) and was used within a day.

SUPPLEMENTAL DATA

Supplemental Data include Supplemental Experimental Procedures, fourteen figures, one table, and sixteen movies and can be found with this article online at http://www.cell.com/developmental-cell/supplemental/S1534-5807(09)00392-X.

ACKNOWLEDGMENTS

We thank Monique Arpin, Claudia Almeida, Laurent Blanchoin, Susanne Bolte, Beatà Bugyi, Marie-France Carlier, Philippe Chavrier, Dafne Chirivino, Evelyne Coudrier, Edgar Gomes, Maud Hertzog, Cathy Jackson, Ludger Johannes,

Marko Kaksonen, Christophe Lamaze, Pekka Lappalainen, Andres Lebensohn, Daniel Lévy, Daniel Louvard, Stéphanie Miserey-Lenkei, Guillaume Montagnac, Graça Raposo, Erez Raz, Michal Reichman-Fried, Rajat Rohatgi, Winfried Römer, Klemens Rottner, Aurélien Roux, Dorothy Schafer, Giorgio Scita, Guillaume Van Niel, and Matt Welch for support, insights, and reagents. We greatly acknowledge the Plateforme d'Imagerie Cellulaire et Tissulaire-Infrastructures en Biologie Santé et Agronomie (PICT-IBiSA) and its staff. This work was supported by Fondation pour la Recherche Médicale (INE20071110919), Centre Nationale de la Recherche Scientifique (PEPS), and Agence Nationale pour la Recherche (ANR-08-BLAN-0012-03 and ANR-08-PCVI-0010-03).

Received: January 15, 2009
Revised: June 9, 2009
Accepted: September 23, 2009
Published: November 16, 2009

REFERENCES

Abramoff, M.D., and Viergever, M.A. (2002). Computation and visualization of three-dimensional soft tissue motion in the orbit. IEEE Trans. Med. Imaging *21*, 296–304.

Akin, O., and Mullins, R.D. (2008). Capping protein increases the rate of actin-based motility by promoting filament nucleation by the Arp2/3 complex. Cell *133*, 841–851.

Benesch, S., Lommel, S., Steffen, A., Stradal, T.E., Scaplehorn, N., Way, M., Wehland, J., and Rottner, K. (2002). Phosphatidylinositol 4,5-biphosphate (PIP2)-induced vesicle movement depends on N-WASP and involves Nck, WIP, and Grb2. J. Biol. Chem. *277*, 37771–37776.

Campellone, K.G., Webb, N.J., Znameroski, E.A., and Welch, M.D. (2008). WHAMM is an Arp2/3 complex activator that binds microtubules and functions in ER to Golgi transport. Cell *134*, 148–161.

Cooper, J.A., and Sept, D. (2008). New insights into mechanism and regulation of actin capping protein. Int. Rev. Cell Mol. Biol. *267*, 183–206.

Derivery, E., Lombard, B., Loew, D., and Gautreau, A. (2009). The Wave complex is intrinsically inactive. Cell Motil. Cytoskeleton *66*, 777–790.

Fink, J.K. (2006). Hereditary spastic paraplegia. Curr. Neurol. Neurosci. Rep. *6*, 65–76.

Itoh, T., Erdmann, K.S., Roux, A., Habermann, B., Werner, H., and De Camilli, P. (2005). Dynamin and the actin cytoskeleton cooperatively regulate plasma membrane invagination by BAR and F-BAR proteins. Dev. Cell *9*, 791–804.

Kaksonen, M., Peng, H.B., and Rauvala, H. (2000). Association of cortactin with dynamic actin in lamellipodia and on endosomal vesicles. J. Cell Sci. *113*, 4421–4426.

Lai, F.P., Szczodrak, M., Block, J., Faix, J., Breitsprecher, D., Mannherz, H.G., Stradal, T.E., Dunn, G.A., Small, J.V., and Rottner, K. (2008). Arp2/3 complex interactions and actin network turnover in lamellipodia. EMBO J. *27*, 982–992.

Linardopoulou, E.V., Parghi, S.S., Friedman, C., Osborn, G.E., Parkhurst, S.M., and Trask, B.J. (2007). Human subtelomeric WASH genes encode a new subclass of the WASP family. PLoS Genet. *3*, e237.

Liu, A.P., and Fletcher, D.A. (2006). Actin polymerization serves as a membrane domain switch in model lipid bilayers. Biophys. J. *91*, 4064–4070.

Liu, J., Kaksonen, M., Drubin, D.G., and Oster, G. (2006). Endocytic vesicle scission by lipid phase boundary forces. Proc. Natl. Acad. Sci. USA *103*, 10277–10282.

Liu, R., Abreu-Blanco, M.T., Barry, K.C., Linardopoulou, E.V., Osborn, G.E., and Parkhurst, S.M. (2009). Wash functions downstream of Rho and links linear and branched actin nucleation factors. Development *136*, 2849–2860.

Loisel, T.P., Boujemaa, R., Pantaloni, D., and Carlier, M.F. (1999). Reconstitution of actin-based motility of *Listeria* and *Shigella* using pure proteins. Nature *401*, 613–616.

Maxfield, F.R., and McGraw, T.E. (2004). Endocytic recycling. Nat. Rev. Mol. Cell Biol. *5*, 121–132.

Mejillano, M.R., Kojima, S., Applewhite, D.A., Gertler, F.B., Svitkina, T.M., and Borisy, G.G. (2004). Lamellipodial versus filopodial mode of the actin nanomachinery: pivotal role of the filament barbed end. Cell *118*, 363–373.

Pantaloni, D., Boujemaa, R., Didry, D., Gounon, P., and Carlier, M.F. (2000). The Arp2/3 complex branches filament barbed ends: functional antagonism with capping proteins. Nat. Cell Biol. *2*, 385–391.

Pollard, T.D. (2007). Regulation of actin filament assembly by Arp2/3 complex and formins. Annu. Rev. Biophys. Biomol. Struct. *36*, 451–477.

Roux, A., Cuvelier, D., Nassoy, P., Prost, J., Bassereau, P., and Goud, B. (2005). Role of curvature and phase transition in lipid sorting and fission of membrane tubules. EMBO J. *24*, 1537–1545.

Roux, A., Uyhazi, K., Frost, A., and De Camilli, P. (2006). GTP-dependent twisting of dynamin implicates constriction and tension in membrane fission. Nature *441*, 528–531.

Schroer, T.A. (2004). Dynactin. Annu. Rev. Cell Dev. Biol. *20*, 759–779.

Takano, K., Toyooka, K., and Suetsugu, S. (2008). EFC/F-BAR proteins and the N-WASP-WIP complex induce membrane curvature-dependent actin polymerization. EMBO J. *27*, 2817–2828.

Takenawa, T., and Suetsugu, S. (2007). The WASP-WAVE protein network: connecting the membrane to the cytoskeleton. Nat. Rev. Mol. Cell Biol. *8*, 37–48.

Tsujita, K., Suetsugu, S., Sasaki, N., Furutani, M., Oikawa, T., and Takenawa, T. (2006). Coordination between the actin cytoskeleton and membrane deformation by a novel membrane tubulation domain of PCH proteins is involved in endocytosis. J. Cell Biol. *172*, 269–279.

Valdmanis, P.N., Meijer, I.A., Reynolds, A., Lei, A., MacLeod, P., Schlesinger, D., Zatz, M., Reid, E., Dion, P.A., Drapeau, P., et al. (2007). Mutations in the KIAA0196 gene at the SPG8 locus cause hereditary spastic paraplegia. Am. J. Hum. Genet. *80*, 152–161.

Zerial, M., and McBride, H. (2001). Rab proteins as membrane organizers. Nat. Rev. Mol. Cell Biol. *2*, 107–117.

Zuchero, J.B., Coutts, A.S., Quinlan, M.E., Thangue, N.B., and Mullins, R.D. (2009). p53-cofactor JMY is a multifunctional actin nucleation factor. Nat. Cell Biol. *11*, 451–459.